Emergence of pediments, tors, and piedmont junctions from a bedrock weathering–regolith thickness feedback

Mark W. Strudley
A. Brad Murray
P.K. Haff

Division of Earth and Ocean Sciences, Nicholas School of the Environment and Earth Sciences, and Center for Nonlinear and Complex Systems, Duke University, Durham, North Carolina 27708, USA

ABSTRACT

Sediment erosion laws form the basis for most landscape evolution models and guide geomorphologists in the pursuit of understanding how landscapes evolve. This focus on the alluvial surface, however, ignores the role of intrinsic feedbacks between sediment transport and bedrock weathering in shaping Earth's landforms. Here, we present a new, parsimonious explanation for the origin and maintenance of pediments, piedmont junctions, and tors, which emerge spontaneously in a numerical model coupling bedrock weathering and sediment transport. The spatial uniformity of the thin regolith mantle that often characterizes pediments is a manifestation of a negative feedback between bedrock weathering and regolith thickness: if regolith thins (thickens) by sediment transport, the regolith production rate will increase (decrease), maintaining an equilibrium regolith thickness on the piedmont. We propose that high infiltration capacities and the instability of ephemeral channel banks in arid and semiarid environments suppress fluvial incision and promote the smoothness of pediments. A positive feedback between bedrock weathering and regolith thickness causes tor growth: if regolith thins locally below a critical value, regolith production slows while surrounding areas continue to weather and erode more rapidly. We suggest that many pedimented and tor-studded landscapes may therefore be a consequence of intrinsic sediment transport–weathering feedbacks mediated by climatic and tectonic conditions, not by lithologic templates.

Keywords: pediments, tors, regolith, weathering, deserts.

INTRODUCTION

Piedmonts, low-relief mountain passes, and regolith-covered domes in arid and semiarid environments often exhibit smooth, low-sloping erosional bedrock surfaces mantled by a thin to nonexistent, spatially uniform regolith blanket, which defines these surfaces as pediments. The bedrock floor of these pediment surfaces (Cooke et al., 1993; Dohrenwend, 1994; Gilbert, 1877; Howard, 1942; McGee, 1897; Sharp, 1957) may protrude through the regolith mantle, ornamenting an otherwise featureless piedmont with complex bedrock exposures known as tors. The transition between pediments and adjoining rocky mountain masses is often abrupt, forming a sharp slope discontinuity, the piedmont junction, despite the absence of faulting or lithologic variability (Dohrenwend, 1994; Oberlander, 1974). The curious and ubiquitous nature of this landform suite (Fig. 1A) has baffled geologists for over a century and highlights the need for a more comprehensive understanding of mountain and piedmont development in these environments.

Sediment transport and erosion on pediments is predominantly caused by stream flow (Dohrenwend, 1994). One explanation for the origin of pediment surfaces points to the action of laterally migrating streams eroding bedrock and leaving a beveled surface (Cooke et al., 1993; Gilbert, 1877; Howard, 1942; Johnson, 1931). However, the extension of pediment surfaces to piedmont junctions would require streams to flow parallel to contours in order to corrade planar mountain fronts. Exposed bedrock on pediments lacks evidence of fluvial sculpting and exhibits rough surfaces characteristic of grain-by-grain spallation via weathering. In addition, pediment morphology contrasts with landscapes carved by streams. Fluvial erosion typically roughens a surface and forms incised drainage networks because of flow concentration downstream and the nonlinear relationship between sediment transport and flow strength (Vanoni, 1975). But many pediments are smooth and are only weakly incised by immature drainage networks characterized by subtle channels (centimeter- to decimeter-scale depth; decimeter- to meter-scale width) that are often observed to fade within tens of meters without connecting to a larger drainage network or contacting bedrock (Boring, 1999; Sharp, 1957; Vincent and Sadah, 1995).

We hypothesize that lateral bank instability (Nichols et al., 2002), aided by sparsely vegetated, noncohesive sediment in the desert environments considered here, contributes to the smoothness of pediments and can allow flows to bifurcate and effectively widen downslope so that water discharge per unit channel width increases less rapidly than in a corresponding channel of constant width. In addition, where convective, localized storms are important (as in many desert environments), high infiltration rates are especially effective at reducing runoff magnitude and flow distance, reducing downstream flow concentration. Finally, the presence of noncohesive soils promotes slope-driven, nonfluvial sediment transport driven by rain splash, which tends to fill in rills and

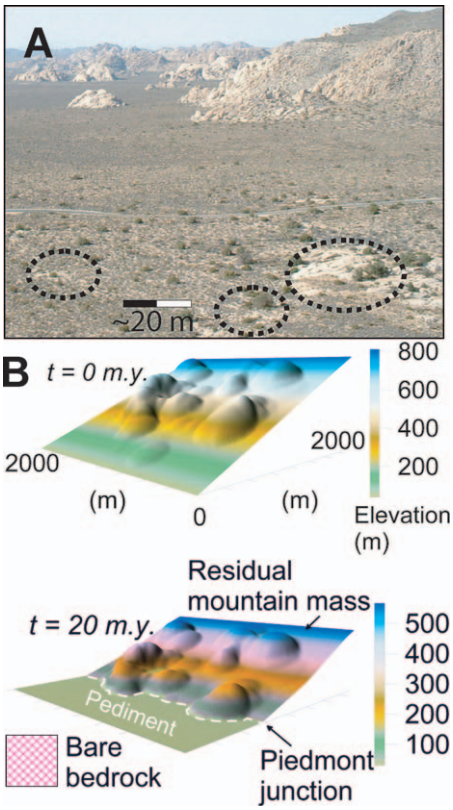

Figure 1. Oblique views of modeled and natural pediments, piedmont junctions, and tors. A: Pediment, piedmont junction, and tors in Joshua Tree National Park, California, USA. Low-lying granitic outcrops (dashed ellipses) in foreground show proximity of bedrock to surface. Pediment basin is hydrologically open; runoff drains toward left foreground. B: An initial bedrock surface consisting of randomly placed irregularities superimposed on an overall planar slope (Appendix DR1, methods [see text footnote 1]), with an open-basin boundary condition, leads to downslope pediment and piedmont junction (dotted line) formation.

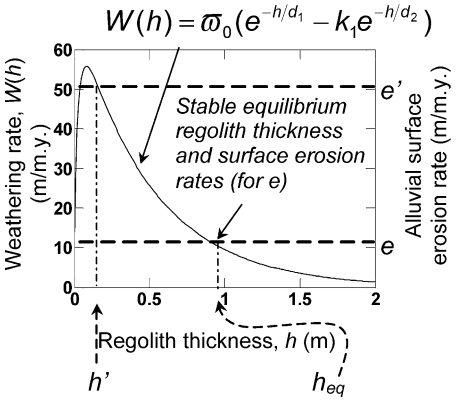

Figure 2. Weathering rate, *W*(*h*) (m/m.y.) as a function of regolith thickness, *h* (m). Dashed lines represent alluvial surface lowering rates (labeled *e* and *e*′ [m/m.y.]). Here, the bare-bedrock weathering rate is 14 m/m.y., and *h* and *h*′ represent stable equilibrium regolith thicknesses.

incipient channels in many arid and semiarid environments (Dunne and Aubry, 1986).

Pediments have also been described as inactive remnants of ancient (Tertiary) weathering profiles (Oberlander, 1974), exposed through subsequent regolith stripping events. However, this hypothesis fails to explain how a uniformly thin regolith layer would be preserved across extensive pediments, and is not consistent with evidence that pediment formation has persisted into the Quaternary (Dohrenwend, 1994). Here we propose that interplay between weathering and sediment transport produces the thin and persistent sediment cover that characterizes pediments and can also cause the growth of tors. Figure 2 represents this graphically: it plots a hypothesized regolith production rate, $W(h)$ (m/m.y.) as a function of regolith thickness, h (m), together with alluvial surface erosion rates (labeled e and e' [m/m.y.]), and illustrates the development of a persistent equilibrium regolith thickness (h_{eq}) on pediments through examination of perturbations about h_{eq}. Note that the particular erosion rates depicted are arbitrary and will be determined by sediment flux divergence and boundary conditions. For $h > h_{eq}$, sediment surface erosion rates are greater than bedrock weathering rates, and thus regolith profiles thin over time. This thinning causes bedrock weathering to accelerate, resulting in an equilibrium regolith thickness ($h \rightarrow h_{eq}$, from right). For $h < h_{eq}$, regolith profiles thicken over time, causing bedrock weathering rates to decrease, and regolith thickness ultimately becomes stable ($h \rightarrow h_{eq}$, from left). Another stable, equilibrium regolith thickness at $h_{eq} = 0$ m derives from the same mechanism, operating to the left of the hump in the weathering curve. The ''humped'' part of the curve is not relevant for pediment development in the model, but plays a role in tor formation.

SIMULATIONS OF PEDIMENT DEVELOPMENT

We illustrate the emergence of pediments, piedmont junctions, and tors by incorporating sediment transport and regolith-thickness–dependent bedrock weathering on desert piedmonts in a numerical model. We employ a regolith production rule (Fig. 2) of the form:

$$W(h) = \varpi_o(e^{-h/d_1} - k_1 e^{-h/d_2}), \quad (1)$$

where $\varpi_o = 70$ m/m.y., $d_1 = 0.5$ m and $d_2 = 0.03$ m are decay scaling factors, and $k_1 = 0.8$ is a dimensionless coefficient that determines the magnitude of the bare-bedrock weathering rate relative to ϖ_o (Granger et al., 1996). The form of the weathering curve is motivated by field observations that suggest that a limited regolith cover enhances the weathering rate relative to bare bedrock (Anderson, 2002; Carson and Kirkby, 1972; Dietrich et al., 2003; Gilbert, 1877), highlighting the importance of mineral hydration and chemical weathering afforded by water retention in thin layers of regolith cover (Oberlander, 1972; Wahrhaftig, 1965).

Our model routes surface runoff across a grid of cells with a resolution much larger (25 m) than typical channel dimensions. The model discharges represent summations over the total discharges in channels that are implicit within each cell (Howard, 1994). We treat sediment erosion and accretion as if they were distributed evenly throughout a cell, reflecting the long time scales of the model (Howard, 1994) and the tendency for channels on pediments to migrate laterally (Nichols et al., 2002). Because we do not resolve individual channels, we must relate sediment flux to aggregated discharges within each cell. The ability of ephemeral channels with unstable banks to widen as flow increases implies that the relationship between sediment transport and bulk discharges is closer to linear than would be the case for within-channel specific discharges. To capture this effect, as well as the high infiltration rates that we suggest contribute to weakly integrated drainage networks on desert piedmonts, we use a weakly nonlinear fluvial transport rule calibrated to produce only shallow incision (Carson and Kirkby, 1972; Howard, 1994):

$$q_{s,f} = k_2 q_w{}^{\alpha} S^{\beta}, \quad (2)$$

where $q_{s,f}$ is the volumetric sediment flux per unit width per storm (m^2/storm), k_2 is a transport efficiency parameter, q_w is the volumetric runoff per unit (cell) width per storm (m^2/storm), S is slope between the centers of adjacent cells, and α and β are constants ($k_2 = 1 \times 10^{-3}$ m$^{2-2\alpha}$/storm$^{(\alpha-1)}$, $\alpha = 1.1$, $\beta = 1$). The infrequent but geomorphically effective storms occurring in these environments on an annual basis (0.10 m/h; 1.0 h/storm; 4 storms/yr; [NOAA, 1999]) determine q_w, which is subsequently modulated by infiltration according to a rearrangement of the Green-Ampt equation (Bedient and Huber, 1992) (see GSA Data Repository[1] for more detail on our infiltration algorithm). The model omits fluvial bedrock incision in accordance with field observations suggesting its lack of importance in modifying bedrock surfaces. We include topographic diffusion—sediment transport that depends on slope but not on discharge (see GSA Data Repository material [see footnote 1])—to simulate small-scale smoothing processes such as rain splash. We calibrated our fluvial transport efficiency parameter so that the relief between swales and subtle interfluves is on the order of a meter, as we have observed on Mojave Desert pediments, and the overall pediment lowering rate is ~10 m/m.y. (Dohrenwend, 1994).

With this sediment transport relationship, spatially averaged fluvial erosion is essentially an efficient large-scale diffusion mechanism that tends to produce a smooth, unincised surface. To test the sensitivity to the form of our fluvial sediment transport rule, we performed model experiments using multiple localized storms with spatially limited runoff. These conditions also produce a lack of significant incision at large scales, even when the transport law is highly nonlinear (Fig. DR9, see footnote 1). Coupled with this fluvial smoothing, the weathering mechanism produces the thin (**O** [m]), uniform regolith blanket characteristic of pediments. In our model and in nature, the pediment regolith in its upper portion consists of stratified, clay-poor, porous, stream-deposited sediment produced by weathering upstream, which is underlain by a weathered soil horizon (Nichols et al., 2002) (except where streams have scoured to bedrock).

A wide range of initial topographies, including irregular mountain masses, can evolve to a pediment (Fig. 1B). However, to most clearly illustrate the evolution of pediments and piedmont junctions, we use here a simplified initial geometry—a steep, inclined, planar bedrock surface (Fig. 3A). Weathering of the initially bare range front produces debris. For steep bedrock slopes (~>5°), runoff

[1]GSA Data Repository item 2006178, methods and Figures DR1–DR12 (attracting pediment morphology and supplementary model simulations), is available online at www.geosociety.org/pubs/ft2006.htm, or on request from editing@geosociety.org or Documents Secretary, GSA, P.O. Box 9140, Boulder, CO 80301, USA.

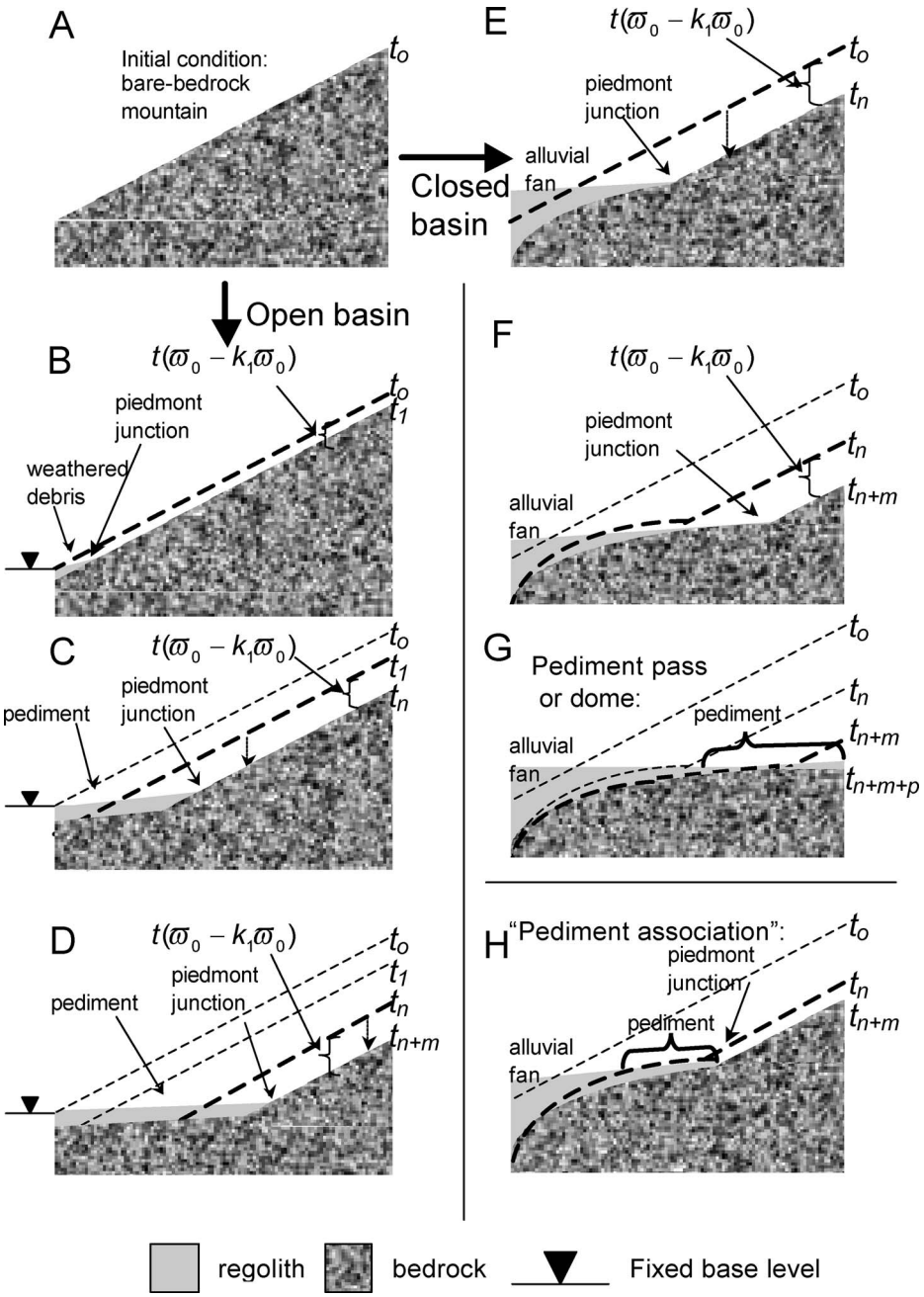

Figure 3. Illustrations of pediment development for both open- and closed-basin boundary conditions (see Fig. DR12 for model results [see text footnote 1]). Bare-bedrock uplands lack topographic detail because of simplified initial conditions and the absence of fluvial bedrock incision in the model. Time steps (*t*) are arbitrary and are used for illustration only; subscripts *n*, *m*, and *p* are used to denote large advances in model time (10^3–10^6 yr), while numeric changes in subscripts (0 to 1) indicate consecutive model time steps. Dashed lines illustrate bedrock surface for previous time step, *t*. Figures are not drawn to scale; regolith thickness (O [m] on pediments) is exaggerated for clarity. A: Initial condition for open- and closed-basin models. B–D: Open-basin pediment development: pediment and piedmont junction form as soon as the foot of the mountain mass retreats from the position of the fixed base level (time steps t_0 to t_1). Headward extension of pediment and piedmont junction continue through time step t_n. E–G: Alluvial fan and pediment development under closed-basin boundary conditions. Following headward migration of a piedmont junction, the mountain mass has eroded completely, leaving a pediment surface upslope and alluvial fan downslope (G). H: Weathering rates an order of magnitude higher, combined with slightly higher rainfall rates (intensity or duration increased by a factor of ~2.5), produce faster-growing pediments and, a "pediment association" (Cooke, 1970) (downslope fan deposit, midslope pediment, and remnant mountain mass).

will tend to remove this debris faster than weathering produces it. Meanwhile, for uniform weathering, the slope of the bare-bedrock mountain mass remains constant as it weathers and retreats (the model omits fluvial bedrock incision). The fate of the debris and evolution of the pediment are determined by downslope boundary conditions. For a hydrologically open basin with a fixed base level (''open'' boundary conditions, Fig. 3A–D), weathered material accumulates at, and upslope of, the fixed base level, creating an alluvial surface with a low slope graded to transport the material delivered to it from the retreating bedrock mass (Fig. 3B). As the mountain mass dwindles and the rate of sediment delivery decreases, the slope and therefore elevation of the alluvial surface decreases, and a pediment forms (Fig. 3C–D). Because the retreating range front remains steep, an abrupt piedmont junction forms where the upslope-propagating pediment intersects the range front.

A hydrologically closed (depositional) basin (''closed-basin'' boundary conditions, Figs. 3A, 3E–H) leads to a rising local base level, whereby material weathered from the upslope bare-bedrock mass accumulates downslope in an alluvial fan that aggrades at decreasing rates as the weathering mountain mass is consumed (Figs. 3E and 3F). Sediment continues moving downslope following the total disintegration of the mountain mass, at which point, the sediment surface begins to erode upslope while aggrading downslope. This transition, in which the upslope portion of a previously depositional surface becomes erosional, allows bedrock weathering and sediment erosion rates to equilibrate, producing a pediment upslope (Fig. 3G). If the upslope portion of the sediment surface begins to erode before the mountain mass vanishes, a piedmont junction will again develop, as in the open-basin simulation (Fig. 3H).

Under both boundary conditions, pediments will ultimately extend to the topographic crest as the mountain mass is removed. This long-term state corresponds to a pediment pass (if the pediment extends upslope to a divide between mountain mass remnants) or dome (in the absence of any remnants), both of which are common in the deserts of the southwestern United States. Prominent examples include Cima Dome, California (Sharp, 1957), pediment passes in the Sacaton Mountains, Arizona (Parsons and Abrahams, 1984), and pediment passes and domes in Joshua Tree National Park, California.

Model experiments suggest that bare-bedrock pediments observed in nature likely reflect pedimentation under open or closed boundary conditions, followed by base-level

incision in which the regolith mantle is stripped, leaving an expansive bedrock bench beneath the foot of mountains (Fig. DR10, see footnote 1).

Our choice of weathering rate does not qualitatively affect pediment development; only modest adjustments to pediment slope (few degrees) occur for ω_o spanning 1–100 m/m.y. Numerous workers have determined that the regolith (soil) production curve in many environments exhibits a monotonic decline in weathering rates with increasing regolith thickness (e.g., Heimsath et al., 1997). These conditions preclude tor growth, but do not prevent the development of an equilibrium regolith thickness, because the regolith-stabilizing feedback is associated with the decaying portion of the regolith production curve (Fig. 2).

EMERGENT LANDSCAPE FEATURES

In our model, the piedmont junction reflects an emergent threshold in erosion styles; mountain slopes are weathering-limited while pediments are transport-limited. Howard (1994) has modeled erosional slope discontinuities in which detachment-limited stream erosion on hillsides gives way downslope to lower-sloped, transport-limited channels, with the slope discontinuity gradually becoming less distinct as erosion and accumulation proceed. Howard's model does not include weathering of bare-bedrock slopes, a key process in the present model that allows slopes to retreat without change of shape, preserving the sharp angular discontinuity.

The peaked nature of the weathering curve provides a mechanism for the growth of isolated tors on an erstwhile smooth pediment. If the sediment erosion rate at some stage of pediment development happens to be greater than the bare-bedrock weathering rate but less than the weathering rate at the peak of the curve (line e' in Fig. 2), then local thinning of the regolith blanket, for example by an especially intense storm cell and concentrated runoff, can cause the system to move toward $h = 0$ (Fig. 2). The exposed bedrock will then lower more slowly than the surrounding pediment plain, forming a free-standing tor with sharply defined edges analogous to piedmont junctions (Fig. DR11, see footnote 1). As the pediment slope slowly declines with time, the sediment erosion rate will eventually fall below the bare-bedrock weathering rate, leading to the eventual disappearance of tors in favor of a featureless pediment surface.

CONCLUSION

The results described here provide a new picture of pediment, piedmont junction, and tor development in which weathering, infiltration, and sediment transport combine to generate these autogenic landforms. This suite of landscape features self-organize in our model in the sense that they arise from the interactions within the system; there is no external template that dictates their existence or spatial arrangement. Especially under open-basin boundary conditions, the emergence of pediments punctuated by much steeper bedrock masses occurs under a wide range of weathering rates, sediment transport parameter values, storm types, and initial geometries (Figs. DR1–DR9, see footnote 1). Adding spatial heterogeneity in weathering rates, representing variations in lithological properties, affects the details of the resulting patterns, but not the basic behaviors; pediments and piedmont junctions still form, and the locations of the junctions do not generally correspond with the boundaries between different weathering rates (lithologies) (Figs. DR6–DR8, see footnote 1).

Pediments and piedmont junctions are common and conspicuous in arid regions because aridity limits weathering rates and vegetation, promotes bare-bedrock uplands, and often provides the conditions for weakly consolidated soils, high infiltration capacities, and localized storm footprints that favor diffusive smoothing by fluvial processes.

ACKNOWLEDGMENTS

We thank members of the Surface Processes Club at Duke University for discussions that stimulated this work. The United States Army Research Office [DAAD19-99-1-0191] and the Andrew W. Mellon Foundation provided partial support.

REFERENCES CITED

Anderson, R.S., 2002, Modeling the tor-dotted crests, bedrock edges, and parabolic profiles of high alpine surfaces of the Wind River Range, Wyoming: Geomorphology, v. 46, p. 35–58, doi: 10.1016/S0169-555X(02)00053-3.

Bedient, P.B., and Huber, W.C., 1992, Hydrology and floodplain analysis: Reading, Massachusetts, Addison-Wesley Publishing Co., 692 p.

Boring, L., 1999, An empirical model of large scale sediment transport in arid terrain [M.S. thesis]: Durham, Duke University, 149 p.

Carson, M.A., and Kirkby, M.J., 1972, Hillslope form and process: New York, Cambridge University Press, 475 p.

Cooke, R.U., 1970, Morphometric analysis of pediments and associated landforms in the western Mojave Desert, California: American Journal of Science, v. 269, p. 26–38.

Cooke, R.U., Warren, A., and Goudie, A., 1993, Desert geomorphology: London, UCL Press, 526 p.

Dietrich, W.E., Bellugi, D.G., Sklar, L.S., Stock, J.D., Heimsath, A.M., and Roering, J.J., 2003, Geomorphic transport laws for predicting landscape form and dynamics, *in* Wilcock, P.R., and Iverson, R.M., eds., Prediction in geomorphology: American Geophysical Union Geophysical Monograph 135, p. 103–132.

Dohrenwend, J.C., 1994, Pediments in arid environments, *in* Abrahams, A.D., and Parsons, A.J., eds., Geomorphology of desert environments: London, Chapman and Hall, p. 321–353.

Dunne, T., and Aubry, B.F., 1986, Evaluation of Horton's theory of sheetwash and rill erosion on the basis of field experiments, *in* Abrahams, A.D., ed., Hillslope processes: Boston, Allen & Unwin, p. 31–53.

Gilbert, G.K., 1877, Report on the geology of the Henry Mountains, U.S. Geographical and Geological Survey of the Rocky Mountain Region: Washington, D.C., U.S. Department of the Interior, 170 p.

Granger, D.E., Kirchner, J.W., and Finkel, R., 1996, Spatially averaged long-term erosion rates measured from in situ produced cosmogenic nuclides in alluvial sediment: The Journal of Geology, v. 104, p. 249–257.

Heimsath, A.M., Dietrich, W.E., Nishiizumi, K., and Finkel, R.C., 1997, The soil production function and landscape equilibrium: Nature, v. 388, p. 358–361, doi: 10.1038/41056.

Howard, A.D., 1942, Pediment passes and the pediment problem: Journal of Geomorphology, v. 5, p. 3–32, 95–136.

Howard, A.D., 1994, A detachment-limited model of drainage basin evolution: Water Resources Research, v. 30, p. 2261–2285, doi: 10.1029/94WR00757.

Johnson, D.W., 1931, Planes of lateral corrasion: Science, v. 73, p. 174–177.

McGee, W.J., 1897, Sheetflood erosion: Geological Society of America Bulletin, v. 8, p. 87–112.

Nichols, K.K., Bierman, P.R., Hooke, R.L., Clapp, E.M., and Caffee, M., 2002, Quantifying sediment transport on desert piedmonts using ^{10}Be and ^{26}Al: Geomorphology, v. 45, p. 105–125, doi: 10.1016/S0169-555X(01)00192-1.

Oberlander, T.M., 1972, Morphogenesis of granitic boulder slopes in the Mojave Desert, California: The Journal of Geology, v. 80, p. 1–20.

Oberlander, T.M., 1974, Landscape inheritance and the pediment problem in the Mojave Desert of Southern California: American Journal of Science, v. 274, p. 849–875.

Parsons, A.J., and Abrahams, A.D., 1984, Mountain mass denudation and piedmont formation in the Mojave and Sonoran Deserts: American Journal of Science, v. 284, p. 255–271.

Sharp, R.P., 1957, Geomorphology of Cima Dome, Mojave Desert, California: Geological Society of America Bulletin, v. 68, p. 273–290.

Vanoni, V.A., 1975, Sedimentation engineering: ASCE Manuals and Reports on Engineering Practice, No. 54: New York, American Society of Civil Engineers, p. 745.

Vincent, P., and Sadah, A., 1995, Fabric analyses of some Saudi Arabian pediment gravels: Journal of Arid Environments, v. 30, p. 371–384.

Wahrhaftig, C., 1965, Stepped topography of the southern Sierra Nevada, California: Geological Society of America Bulletin, v. 76, p. 1165–1190.

Manuscript received 30 November 2005
Revised manuscript received 7 April 2006
Manuscript accepted 25 April 2006

Printed in USA